Available online at www.sciencedirect.com
SCIENCE DIRECT
Polymer 46 (2005) 6064–6074
polymer
www.elsevier.com/locate/polymer

Dielectric spectroscopy using dielectric probes: a new approach to study glass transition dynamics in immiscible apolar polymer blends

W.G.F. Sengers[a,b], O. van den Berg[a,b], M. Wübbenhorst[a,*], A.D. Gotsis[b,c], S.J. Picken[a,b]

[a]*Polymer Materials and Engineering, Faculty of Applied Sciences, Delft University of Technology, Julianalaan 136, 2628 BL Delft, The Netherlands*
[b]*Dutch Polymer Institute (DPI), P.O. Box 902, 5600 AX Eindhoven, The Netherlands*
[c]*Department of Sciences, Technical University of Crete, University Campus, GR-73100 Chania, Greece*

Received 17 January 2005; received in revised form 19 April 2005; accepted 21 April 2005
Available online 17 June 2005

Abstract

Dielectric relaxation spectroscopy using dielectric probes was applied to study the (glass transition) dynamics in binary blends of isotactic PP, PS and LDPE. The blends were prepared by melt-mixing and doped with 0.5% of the dielectric probe 4,4′-(*N*,*N*-dibutylamino)-(*E*)-nitrostilbene (DBANS) (van den Berg O, Sengers WGF, Jager WF, Picken SJ, Wübbenhorst M. Macromolecules 2004;37:2460. [17]). Due to the selective amplification of the dielectric relaxation processes related to the dynamic glass transition of the polymers, accurate relaxation data were obtained, even for the minor phases. No substantial influence of the blend composition and the blend morphology on the glass transition dynamics was found, indicating that both blend constituents behave like homogeneous bulk materials. The normalised relaxation strength of glass transition processes remained constant, regardless of the blend type and blend composition. This indicates that the probe molecule, DBANS, was equally distributed over the two blend components in all three polymer combinations PE–PP, PE–PS and PP–PS.

Keywords: Polymer blends; Dielectric relaxation; Glass transition

1. Introduction

Broadband dielectric relaxation spectroscopy (DRS) is one of the most suitable and versatile techniques to assess the dynamics of polymer materials in a wide dynamic range, which typically covers 10 decades in frequency or time [1–4]. By virtue of probing orientational fluctuations that involve molecular (permanent) dipoles, DRS is able to provide detailed insight in the molecular and cooperative dynamics on various time and length scales. Depending on the particular polymer system, ranging from 'simple' amorphous or semi-crystalline polymers [4–6] to more complex systems like miscible [7–10] and immiscible [7,9–11] polymer blends, liquid-crystalline polymers [12,13], supramolecular polymers [14] and nano-composites, one or more characteristic dielectric relaxation processes are detected, which can be assigned to, e.g. the primary relaxation (usually the α process) associated with the dynamic glass transition[1], or local relaxations involving simple bond rotation processes (β, γ, δ relaxation).

A prerequisite for DRS measurements is the presence of molecular dipoles in the polymer structure. Non-polar polymers like polyethylene and polypropylene do not have appreciable molecular dipoles and are thus not dielectrically active, at least in their pure form. However, these materials can be made accessible to dielectric spectroscopy by introducing polar groups in the structure, which allows the dynamics of the polymer molecules to be detected [15,16].

There are two main routes to achieve this: (1) by chemical modification (labelling) of the polymer structure, e.g. by means of partial oxidation [15,16], chlorination or attachment of pendant groups, or (2) by dissolving of suitable polar probe molecules [17–19] which act as dielectric probes in the polymer matrix. Polyethylene can be made dielectrically active by partially oxidation in the presence of air [15] or catalysed by TiO_2 [16] during melt

* Corresponding author. Tel.: +31 15 2781828; fax: +31 15 2787415.
E-mail address: m.r.wubbenhorst@tnw.tudelft.nl (M. Wübbenhorst).

0032-3861/$ - see front matter © 2005 Elsevier Ltd. All rights reserved.
doi:10.1016/j.polymer.2005.04.095

[1] For semi-crystalline polymers, we consider the dynamic glass transition process as the β process. The α process concerns the intra-crystalline relaxation process.

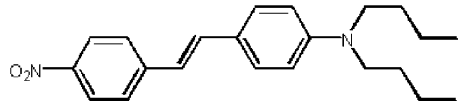

Fig. 1. Chemical structure of 4,4′-(*N*,*N*)-(dibutyldiamino)-(*E*)-nitrostilbene (DBANS).

mixing. These methods, however, are unsuitable for isotactic PP as the oxidation of PP leads to chain scission [20].

In a previous paper we have discussed an alternative approach to 'sensibilise' apolar polymers for studying them by dielectric relaxation spectroscopy, namely by using a dielectric probe at low concentrations [17]. Fig. 1 shows the chemical structure of the dielectric probe molecule used, 4,4′-(*N*,*N*-dibutylamino)-(*E*)-nitrostilbene (DBANS). This molecule was designed to combine a rigid rod-type aromatic core, facilitating a strong dipole moment of $\mu = 9$ D [21] with an aliphatic tail that ensures good solubility in aliphatic matrices and prevents crystallisation of the probe. The high dipole moment allows the doping level to be kept as low as 0.1–0.5 wt%, while maintaining a sufficient dielectric probe response ($\propto \mu^2$).

The crucial question of any (rotator) probe technique is the coupling of the probe fluctuations with molecular motions in its environment. For the case of DBANS, dispersed in polystyrene (PS), polypropylene (PP) and low-density polyethylene (LDPE), it was shown in Ref. [17] that large angular fluctuations of the probe DBANS exclusively couple to the primary relaxation, i.e. the cooperative dynamic glass transition. In other words, the dielectric probe senses the microviscosity in its close vicinity in a correct way.

The present paper aims to extend the dielectric probe technique to the case of binary polymer blends, consisting of two apolar polymers. Starting from the previous results obtained from the homopolymers PS, PP and LDPE, we have investigated three binary blends: PS–PP, PS–PE and PE–PP. As the polarity difference between the two polymer fractions is rather small for all the three blend compositions, it is expected that the probe molecule cannot distinguish between two phases and will thus be present in both phases. The relaxation behaviour of all three blend types will be studied as a function of the blend-type and the blend composition.

2. Experimental

2.1. Materials

The polymers used were polystyrene (PS, Shell N7000), low-density polyethylene (PE, Sabic LDPE 2100TN00) with a melt flow index (MFI) of 0.3 dg/min at 190 °C and 2.16 kg and isotactic polypropylene (PP, DSM Polypropylenes Stamylan 11E10) with a MFI of 0.3 dg/min at 230 °C and 2.16 kg. PS was purified by triple precipitation from dichloromethane/methanol, whereas the PP and PE grades were used as received. Details about the synthesis of the dielectric probe, 4,4′-(*N*,*N*-dibutylamino)-(*E*)-nitrostilbene (DBANS) can be found in Ref. [17].

2.2. Sample preparation

The blends were prepared by melt mixing in an internal batch mixer at 200 °C (Brabender plasticorder 20 cm^3). The polymers were preblended at 100 rpm for 8 min before DBANS was added. After 2 min of continuous mixing, the samples were compression moulded at 200 °C into sheets with a thickness of 0.3 mm. For each blend type, three different blend compositions were made with 75, 50 or 25 wt% of each polymer. The sample coding consists of the polymer abbreviations and their weight percentages, like PS25PE75. All samples contain 0.5 wt% DBANS.

2.3. Scanning electron microscopy

The morphology of the blends was studied with scanning electron microscopy (SEM, Philips XL20). All samples were fractured in liquid nitrogen and sputtered with gold. The acceleration voltage was 15 kV and magnifications from 264× to 2000× were used to observe the blend morphology.

2.4. Dielectric relaxation spectroscopy

To obtain samples with well-defined geometry for DRS experiments, sheets of about 0.3 mm in thickness were heated to 180 °C and pressed together with 100 μm glass fibre between circular brass electrodes ($\varnothing = 2$ cm) followed by rapid cooling under a light pressure ($\sim 10^4$ Pa). Dielectric measurements were performed using a high precision dielectric analyser (ALPHA analyzer, Novocontrol Technologies) in combination with a Novocontrol Quatro temperature system providing control of the sample temperature with high accuracy (uncertaincy < 0.05 K). Temperature dependent experiments were prepared by consecutive isothermal frequency sweeps (10^{-1}–10^7 Hz) in the temperature range from +200 to −120 °C in steps of 5 K, which resulted in an effective cooling rate of about 0.5 K/min. For quantitative evaluation of the relaxation time $\tau(T)$ and other relaxation parameters we fitted the dielectric loss spectra $\varepsilon''(\omega)$ to the empirical Havriliak–Negami (HN) relaxation function (Eq. (1)):

$$\varepsilon'' = -\mathrm{Im}\left\{\frac{\Delta\varepsilon}{(1+(\mathrm{i}\omega\tau)^a)^b}\right\} + \frac{\sigma}{\varepsilon_v\omega} \tag{1}$$

where $\Delta\varepsilon$ and τ correspond to the relaxation strength and the mean relaxation time of the relaxation process. The two shape parameters a and b, which give the logarithmic slope of the low frequency loss tail (a) and the high

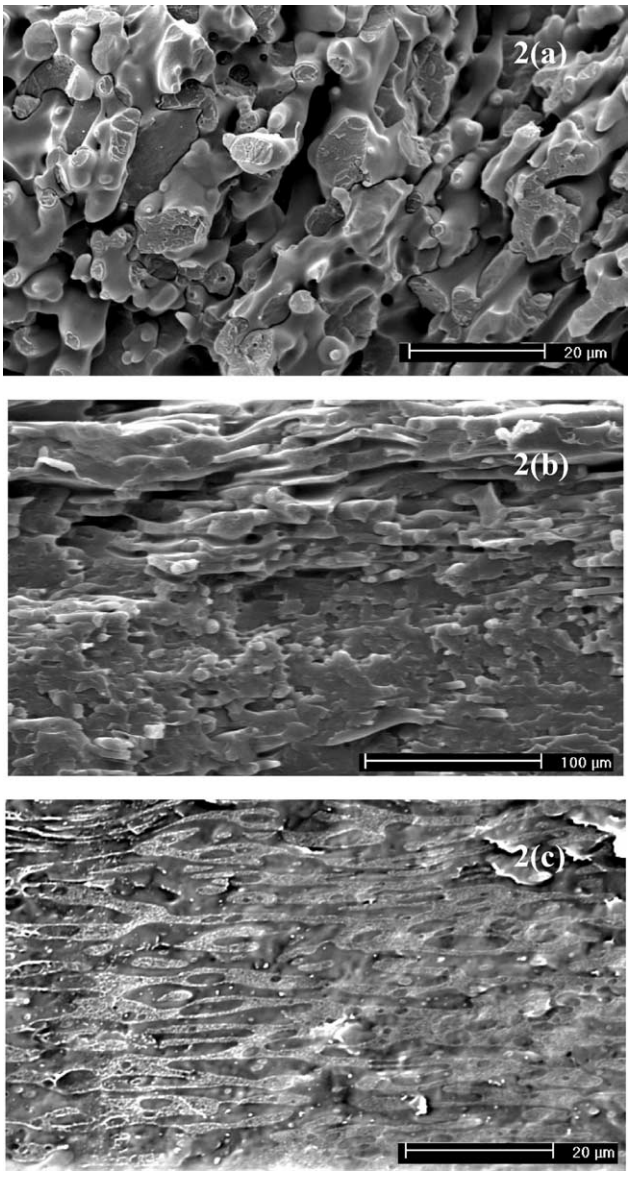

Fig. 2. SEM images of blends at 50–50 compositions. (a) PS50PP50, (b) PS50PE50 and (c) PP50PE50.

frequency loss tail ($-ab$), are determined by the underlying distribution in relaxation times. The second term in Eq. (1) accounts for Ohmic conduction. A comprehensive description of analysis methods for dielectric data can be found in Refs. [22,23].

2.5. Dynamic mechanical analysis

The glass transition temperatures in the pure polymer and their blends were determined by dynamic mechanical analysis (DMA). A Perkin–Elmer DMA 7 was used in tensile mode at a frequency of 1 Hz. The samples were heated from −150 to 200 °C at a rate of 5 °C/min. The mechanical T_g was defined as the maximum in the loss modulus.

2.6. Differential scanning calorimetry

DSC heat flow curves were recorded with a Perkin–Elmer DSC 7. Indium was used for temperature calibration. All samples were annealed for 10 min at 200 °C and subsequently cooled at a rate of 10 K/min to −125 °C. The glass transition temperatures were determined from half ΔC_p values and the crystallisation temperatures from the onset of the crystallisation peak. The degree of crystallinity, X_p, was calculated from the heat of crystallisation of the blend using a linear relation:

$$X_p = \frac{\Delta H_b}{w_p \Delta H_p} \tag{2}$$

where ΔH_b is the heat of crystallisation in the blend and w_p the mass fraction of polymer p. ΔH_p is the heat of crystallisation for polymer p and amounts to 209 J/g for PP and 290 J/g for PE [24].

3. Results and discussion

3.1. Morphology

The phases in the binary blends show typical length scales in the order of 1–30 μm. As expected, the morphology in the binary blends changes with the composition and the polymers used. Because the polymers have comparable viscosities during mixing (similar melt flow indices), the phase inversion point is expected to be around 50 wt% in all blends. Fig. 2 shows SEM images of the three 50/50 blends. In all the three blend types the two phases show layered structures in which the two phases appear to be continuous. Apart from the 50/50 blends, different structure evolution was found upon changing the composition in the blends. The final morphology depends also on the interfacial tension and the processing conditions [25–27].

The blend PS25PP75, in which PS is the minor phase, shows a droplet in matrix morphology with PS domains of about 4 μm. At 50 wt% PS (Fig. 2(a)), both phases seem to be continuous with an average striation size of 5 μm, while for the blend containing 75 wt% PS the morphology reveals a combination of oriented PP sheets (ca. 10×30 μm^2) and smaller PP droplets (1–3 μm).

The blends of PE and PS show a structural evolution from sheets of PS (5×20 μm^2) in a PE matrix for PS25PE75 to a co-continuous layered structure of the two phases for PS50PE50 (Fig. 2(b)), to sheet morphology of PE in a PS matrix for PS75PE25.

For the PP–PE blends, the morphology of PP25PE75 consists of a fine dispersion of rod like PP particles of 0.5×2 μm^2. At 50 wt% PP co-continuous structures are present (Fig. 2(c)) with striation sizes of 3 μm, this changes into

Table 1
Glass transition temperatures and crystallisation characteristics measured by DSC

	Glass transition			PP crystallisation			PE crystallisation		
	T_g PS (°C)	T_g PP (°C)	T_g PE (°C)	T_c[a] (°C)	ΔH (J/g)	X_{PE}[b]	T_c[a] (°C)	ΔH (J/g)	X_{PE}[c]
PS	96.3								
PP		−8.8		112.7	−91.6	0.44			
PE			−31.1				97.9	−77.0	0.27
PS25PP75	[d]	[d]		114.1	−71.8	0.46			
PS50PP50	96.5	[d]		115.6	−46.9	0.45			
PS75PP25	96.4	[d]		114.0	−18.6	0.36			
PS25PE75	[e]		[d]				96.6	−57.5	0.26
PS50PE50	[e]		[d]				96.4	−38.3	0.26
PS75PE25	[e]		[d]				97.6	−15.5	0.21
PP25PE75		[d]	[d]	110.2	−6.2	0.11	99.5	−58.9	0.27
PP50PE50		[d]	[d]	118.7	−43.7	0.42	97.6	−28.0	0.19
PP75PE25		−10.1	[d]	117.6	−68.2	0.44	96.8	−12.7	0.17

[a] Onset of crystallisation.
[b] Crystallinity calculated using $\Delta H_{PP}=209$ J/g [14].
[c] Crystallinity calculated using $\Delta H_{PE}=290$ J/g [17].
[d] T_g not observed.
[e] Overlap with crystallisation of PE.

dispersed micron-sized spherical PE domains for composition PP75PE25.

3.2. DSC and DMA

Differential scanning calorimetry (DSC) and dynamic mechanical analysis (DMA) are well-established techniques for the measurement of thermal transitions including the glass transition, and served in this study as reference techniques. A calorimetric glass transition temperature was obtained from the half ΔC_p values of the DSC heat flow curves upon cooling, this yields a T_g value corresponding to a characteristic frequency between 10^{-4} and 10^{-2} Hz, depending on the cooling rate of the experiment and the local activation energy of the structural relaxation. In contrast to DSC, the 'mechanical' glass transition temperature was evaluated from the position of the maximum in the loss modulus, $E''(T)$, at 1 Hz. Due to this difference in the effective measurement frequency, a systematic difference in the T_gs is expected. The results for the glass transition temperatures and crystallisation characteristics are listed in Table 1 (DSC) and Table 2 (DMA). It was not possible to determine meaningful T_g-values in blends in some cases. For PS–PE blends, for example, the glass transition region of the PS phase interferes with the crystallisation temperature window of the PE phase. In the case of PP–PE blends, the changes in the heat capacity were too small to determine the glass transition temperatures of the two phases unambiguously.

The temperature dependent elastic moduli $E'(T)$ and $E''(T)$ of all PS–PP blends and PP–PE blends are summarised in Figs. 3 and 4. Here, Fig. 3(b) reveals two loss maxima corresponding to the glass transition of the PP fraction, $T(\beta_{PP})$, between −11 and −8 °C, and the glass transition of the PS phase, $T(\alpha_{PS})$, around 93 °C. With increasing PS content, the PP loss peak decreases and it is

Table 2
Glass transition temperatures measured by DMA and by DRS

	DMA			DRS[a]		
	T_g PS (°C)	T_g PP (°C)	T_g PE (°C)	T_g PS (°C)	T_g PP (°C)	T_g PE (°C)
PS	93			98.4		
PP		−9			−9.1	
PE			−31			−31.9
PS25PP75	91.2	−9.9		100.3	−14.3	
PS50PP50	88.9	−11.0		101.7	−13.0	
PS75PP25	91.8	−9.3		100.9	−10.0	
PS25PE75	[b]		−35.5	100.4		−33.0
PS50PE50	96.5		−33	100.2		−32.3
PS75PE25	94		−36	99.4		−34.1
PP25PE75		−11.5	−33		−6.0	−32.9
PP50PE50		−9	[b]		−8.1	−34.5
PP75PE25		−12.3	[b]		−11.2	−36.4

[a] $\tau=1$ s.
[b] T_g not observed.

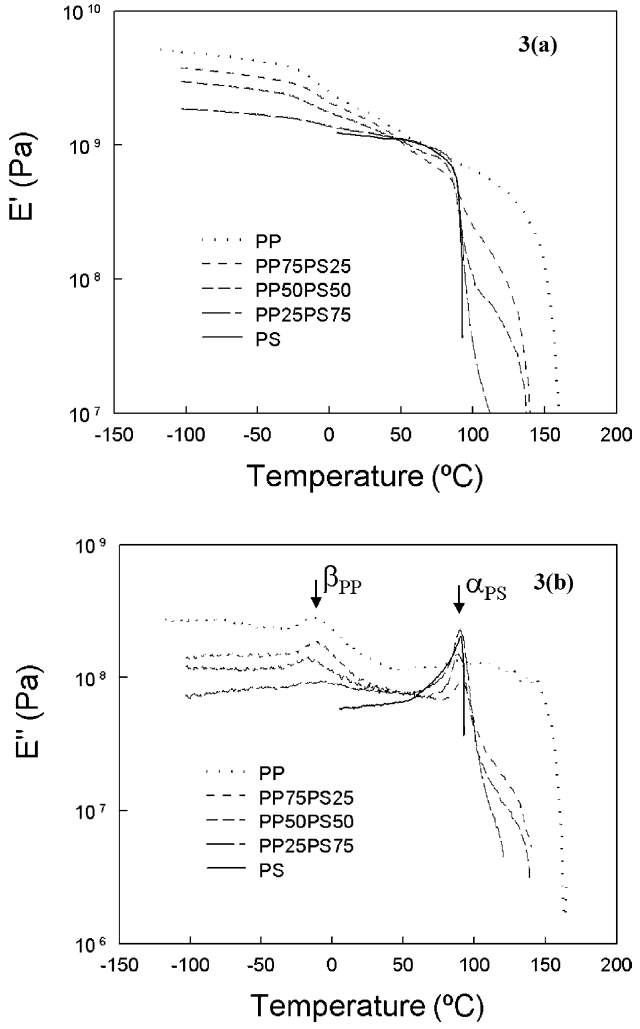

Fig. 3. Storage (a) and loss (b) modulus of PS–PE blends at 1 Hz and 5 °C/min. The arrows indicate the positions the glass transition processes of PS (α_{PS}) and PP (β_{PP}).

broadened in the case where the PP phase is dispersed (blend PS75PP25). In the case of PP–PE blends, the two peaks in the loss modulus partially overlap (Fig. 4(b)). The glass transition dynamics of the PP and PE phases, $T(\beta_{PP})$ and $T(\beta_{PE})$ fall within the range of −40 to 30 °C [24]. In the low temperature range, the sub-glass transition process of PE, γ_{PE}, is present. Its maximum, however, falls outside the temperature range of the experiment. The maxima in $E''(T)$ of the PP phase corresponding to $T(\beta_{PP})$ are located around −10 °C. In the case of the β_{PE} peak in the blends, the maximum in loss modulus (−33 °C) is only observed in the blend containing 75 wt% PE. The curves of the other blends do not show clear maxima, because the β_{PE} peak overlaps strongly with the peak of the PP phase.

3.3. Dielectric relaxation spectroscopy

The two previous sections were aimed to verify the morphology and the fact, that in all cases each polymer phase basically shows its unperturbed bulk behaviour for all blend compositions. This observation is important since we have to realise that all blends contained a mass fraction of 0.5 wt% of the dielectric probe DBANS without showing any substantial effect on the glass transition (DSC, DMA) and the crystallisation behaviour.

We will now focus on the dielectric relaxations of the various blends containing equal amounts of DBANS in order to see in how far the incorporation of dielectric probe molecules helps to study the complex relaxation behaviour of apolar blends in more detail. In a previous paper [17], we demonstrated that addition of DBANS specifically enhances the dielectric relaxation processes associated with the dynamic glass transition, while other processes, viz. local processes in the glassy state and intra-crystalline relaxations are not affected. This specific selectivity for cooperative (segmental) motions in the polymer matrix indicates that there is a good match of the probe length (∼1.3 nm) with the characteristic length scale of the segmental motions (2–5 nm [28]), which results in large angular fluctuations of the stiff probe molecule on the time scale of the dynamic glass transition. Local relaxation processes, in contrast, exhibit typical length scales much shorter than the dynamic glass transition and, hence, do not give room for large angular rotational diffusion of the probe molecules around their short axis.

From the addition of dielectric probes to binary blends of glass forming polymers we expect, to first approximation, a simple additive behaviour of the two polymer fractions with respect to their dielectric response. However, due to the (electrically) inhomogeneous nature of polymer blends and the introduction of an additional superstructure (morphology) on a micrometer scale, one has to consider the following:

(i) The probe molecules might show a different affinity to the two blend constituents, which will result in a preferential location in one of the polymer fractions or at interfaces.
(ii) The proper analysis of dielectric spectra of electrically heterogeneous systems requires the application of mixing rules [29], which account for the shape and interconnectivity of the two-phase system.
(iii) Molecular relaxations might exhibit deviations with respect to their bulk response that originate from the large internal blend interfaces, as well as, from size effects (confinement), particularly if the blend dimensions are far below 1 μm.

As already pointed out in the introduction, we do not expect strong preferential dissolution of the probe in the blends under investigation. The solubility parameters of the polymers are close to each other and the probe should thus be present in both phases of the blend. Due to the aromatic nature of the probe, a slightly higher affinity towards the PS fraction compared to PP or PE is to be expected.

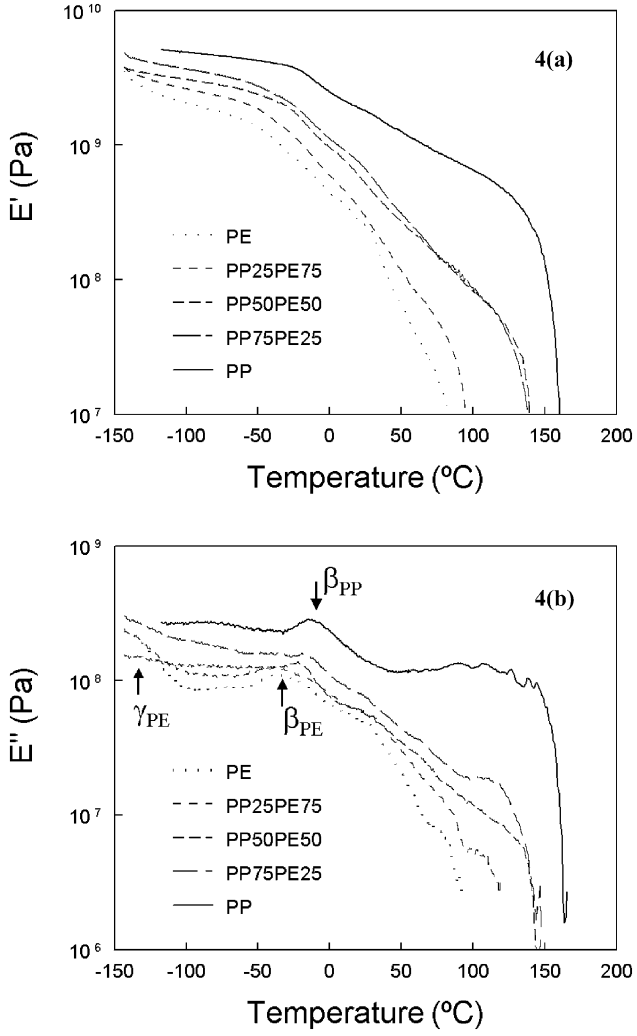

Fig. 4. Storage (a) and loss (b) modulus of PP–PE blends at 1 Hz and 5 °C/min. The arrows indicate the positions of the glass transition processes of PP (β_{PP}) and PE (β_{PE}) and the sub glass transition process in PE (γ_{PE}).

Concerning the dielectric heterogeneity, which in principal could affect the apparent intensity of the dielectric response originating from the two different polymer fractions, we are in the fortunate situation that the relative dielectric permittivity, ε', of the polymers varies only marginally, i.e. $\varepsilon'(\mathrm{PS}) \sim \varepsilon'(\mathrm{PP}) \sim \varepsilon'(\mathrm{PE}) \sim 2.5$. Hence, no morphology dependent mixing rules are required for quantitative data analysis [10]. However, remaining differences in the conductivity might give rise to interfacial relaxations that will be discussed below.

Possible size effects on the molecular relaxations are not substantial, since the blend dimensions (1–20 μm) are still far above typical length scales (~100 nm) for which chain confinement or finite size effects have been reported [30–32].

3.3.1. Identification of relaxation peaks

An overview of the various dielectric relaxation processes is given by Fig. 5, for the dielectric loss, ε'', as a function of temperature and frequency for two blends types. Five relaxation processes can be identified in the blend PS25PE75 (Fig. 5(a)). Two processes originate from the PS fraction: the α process of PS (between 100 and 160 °C) and the secondary β_{PS} process (around −100 °C at $f \sim 1$ kHz). The other three peaks originate from the PE fraction: the intra-crystalline α_{PE} process (high temperature shoulder), the glass transition (β_{PE}) process (the lower and more pronounced peak) in the range −30 to 50 °C, and the γ_{PE} process at around −100 °C. The latter process strongly interferes with the β_{PS} peak.

To confirm this peak assignment, isochronal loss curves $\varepsilon''(T, f=1\ \mathrm{kHz})$ for different PS–PE blend compositions, including the pure blend components, are shown in Fig. 6. With increasing PS content, the relaxation strength of the β_{PE} process decreases gradually, while the relaxation strength of the α_{PS} process shows the reverse trend. In contrast, no shifts in the loss peak maxima related to the dynamic glass transition (i.e. α_{PS} and β_{PE}) are observed, indicating that the two phases retain the glass transition dynamics of the corresponding pure polymers. The glass transition dynamics, thus, is not affected by the blend composition or morphology.

The effect of the blend composition and morphology on the intra-crystalline α_{PE} process and the local relaxations γ_{PE} and β_{PS} is less obvious, since these processes do not benefit from the addition of dielectric probes. We believe that the presence of these relaxation peaks in the dielectric loss is due to slight oxidation of the polymers. Their weak intensities, however, do not allow to judge possible effects of the morphology since this relaxation behaviour might arise from e.g. residual stresses or changes in the crystal dimensions [33].

While the glass transitions of PS and PE phases are well separated, the glass transition regions of the two phases in PP–PE blends strongly overlap. Fig. 5(b) shows the corresponding 3D representation of the dielectric loss of the blend PP50PE50. Between −30 and 65 °C the two β processes of both polymers can be resolved as partially overlapping peaks. The two intra-crystalline processes α_{PE} and α_{PP}, originating from the crystalline PE and PP fractions, are not discernible for any blend composition. The same holds for the local γ-relaxations of the two polymers, which are generally hardly detectable by DRS, and which do not gain intensity upon the addition of DBANS.

A close-up of the overlapping glass transition region of the PP–PE blend is shown in Fig. 7, which shows the β processes of the two polymers in the frequency domain at $T = 10$ °C. With increasing PP content, the intensity of the low-frequency (PE) peak decreases, while the high-frequency (PP) peak becomes stronger. In addition a small shift in the PP relaxation time is observed in all of the blends compared to that of the pure PP.

3.3.2. Mapping of the relaxation times

The relaxation strength and relaxation times were

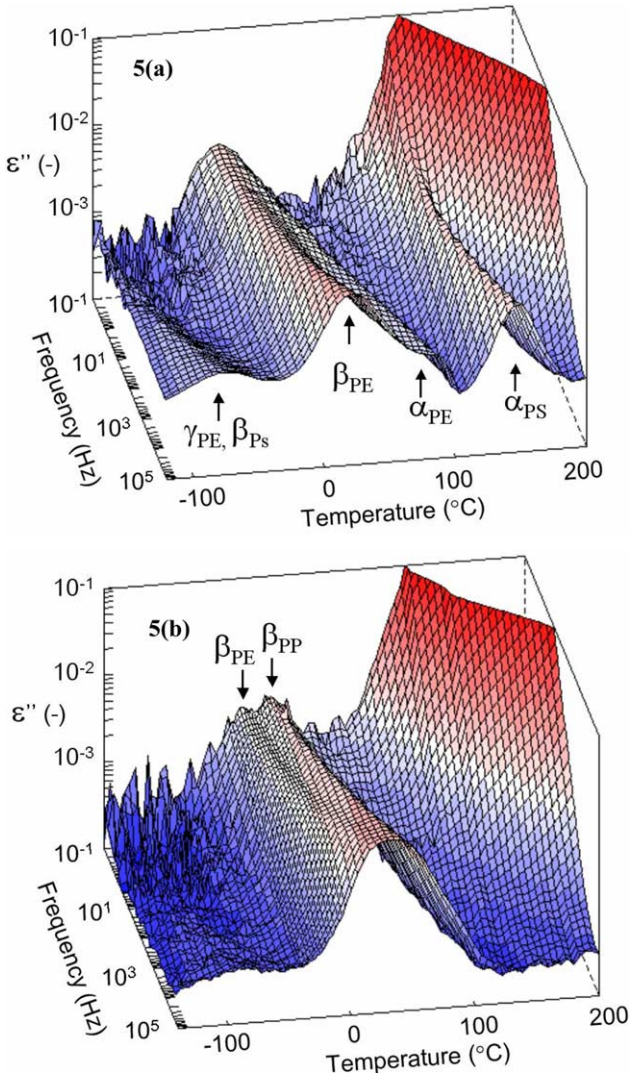

Fig. 5. Dielectric loss as a function of temperature and frequency of (a) PS25PE75 and (b) PP50PE50. The arrows in (a) indicate the position of the intra-crystalline relaxation process in PE (α_{PE}), the glass transition processes of PS (α_{PS}) and PE (β_{PE}) and the sub-glass transition processes of PS (β_{PS}) and PE (γ_{PE}); and in (b) the glass transition processes of PP (β_{PP}) and PE (β_{PE}).

evaluated from the frequency spectra of the dielectric loss using the HN equation (Eq. (1)). To enhance the stability of the fit-procedure, we have set the shape parameter b_{HN}, which accounts for the asymmetry of the loss peak, to a fixed value based on data obtained from the pure polymers. The relaxation time data (corresponding to peak maxima) for the three blend types are given in an Arrhenius representation in Figs. 8–10.

Clearly, all relaxation time data associated with the dynamic glass transition (α_{PS}, β_{PP} and β_{PE}) obey the typical signature of the Vogel–Fulcher–Tammann (VFT) behaviour (Eq. (3)),

$$\tau(T) = \tau_\infty \exp\left(\frac{E_V}{R(T - T_V)}\right) \tag{3}$$

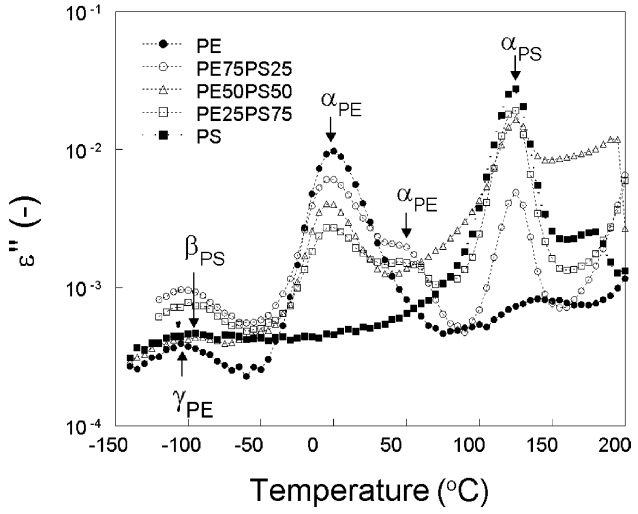

Fig. 6. Temperature dependence of the dielectric loss at 1 kHz for PS–PE blends. The arrows indicate the position of the intra-crystalline relaxation process in PE (α_{PE}), the glass transition processes of PS (α_{PS}) and PE (β_{PE}) and the sub-glass transition processes of PS (β_{PS}) and PE (γ_{PE}).

Here τ_∞ is the pre-exponential factor, E_V is the 'Vogel' energy in kJ/mol, R is the gas constant and T_V is the reference temperature. In contrast, the intra-crystalline α process of PE and the sub T_g processes in PS and PE follow Arrhenius type behaviour:

$$\tau(T) = \tau_\infty \exp\left(\frac{E_a}{RT}\right) \tag{4}$$

where E_a denotes a 'true' Arrhenius activation energy. The experimental findings will now be discussed in detail.

3.3.2.1. PS–PE blends. Fig. 8 shows all relaxation processes found for various PS–PE blends, which can clearly be

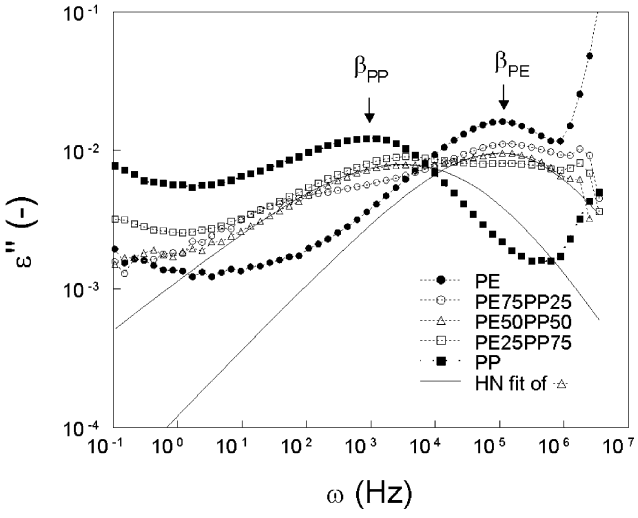

Fig. 7. Frequency dependence of the dielectric loss at 10 °C for PP–PE blends. The lines represent the Havriliak–Negami fits for the PP and PE phases in the blends. The arrows indicate the positions of the glass transition processes of PP (β_{PP}) and PE (β_{PE}).

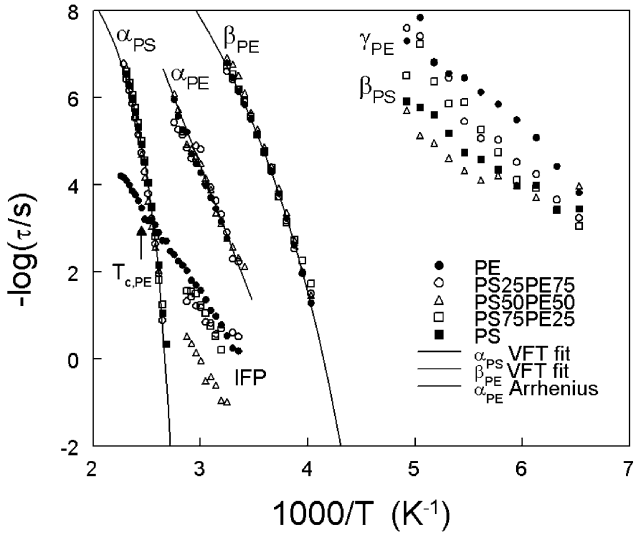

Fig. 8. Logarithm of the relaxation times in PS–PE blends as a function of the inverse temperature. The lines represent the Arrhenius fit of the intra-crystalline relaxation process in PE (α_{PE}) and the VFT fits of the glass transition processes in PS and PE (α_{PS} and β_{PE}). β_{PS} and γ_{PE} are the sub-glass transition relaxation processes in PS and PE, respectively; $T_{c,PE}$ is the crystallisation temperature of PE and IFP means interface polarisation.

assigned to either the PS or the PE fraction. The two glass transition processes β_{PE} and α_{PS}, which can be fitted to the VFT relation (cf. Tables 3 and 5) turn out to be insensitive to variations in the blend composition and thus the blend morphology. Interestingly, the α_{PE} relaxation, being located between the two glass transition processes, shows a similar robustness to variations of the blend composition. This is demonstrated by the marginal variations in the activation energy $E_a(\alpha_{PE})$ between 106 and 120 kJ/mol, which is in agreement with earlier observations from DRS studies [16] and NMR measurements [34]. Such insensitivity of the

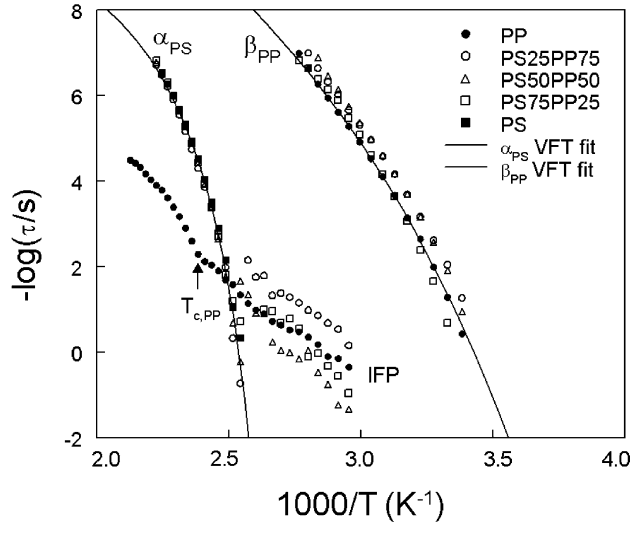

Fig. 9. Logarithm of the relaxation times in PS–PP blends as a function of the inverse temperature. The lines represent the VFT fit of the glass transition processes in PS and PP (α_{PS} and β_{PP}). $T_{c,PE}$ is the crystallisation temperature of PE and IFP means interface polarisation.

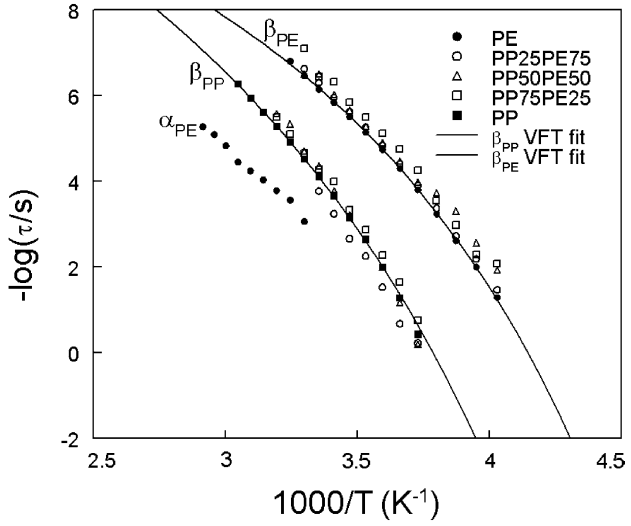

Fig. 10. Logarithm of the relaxation times in PP–PE blends as a function of the inverse temperature. The lines represent the VFT fit of the glass transition processes in PP and PE (β_{PP} and β_{PE}). The intra-crystalline relaxation process of PE (α_{PE}) is included.

intra-crystalline α_{PE} relaxation to morphological changes indicates that the thickness of PE lamellae is insensitive to the blend composition and morphology. Besides the α_{PE} process, another slower relaxation process can be seen in the temperature range from 0.0027 to 0.0033 K^{-1} (90–30 °C). This process exhibits a clear dependence on the blend composition, which is a strong indication for assigning it to interfacial polarisation (IFP). Such process orignates predominantly from differences in the electrical conductivity of the two polymer fractions that lead to charge accumulation and thus charge polarisation at the blend interfaces. For a given morphology, the temperature dependence of the relaxation time $\tau_{IF}(T)$ basically reflects the temperature dependence of the conductivity of the mobile (conductive) fraction (here PE), which typically follows the VFT relation of the structural relaxation time $\tau_{\beta PE}(T)$. Vertical shifting of the IF relaxation data to the VFT fit line of the β_{PE} process, indeed, confirms the common molecular mechanism for the $\tau_{IF}(T)$ and $\tau_{\beta PE}(T)$ data.

At 0.0049 K^{-1} or higher (lower than −70 °C), the secondary β_{PS} and γ_{PE} relaxations are visible. For the pure

Table 3
VFT fit results for PS and its blends

	α_{PS}		
	T_v (K)	E_v (kJ/mol)	log(τ_∞)
PS	317.3	12.7	−12.2
PS25PP75	327.6	9.9	−11.3
PS50PP50	329.8	9.9	−11.5
PS75PP25	324.8	11.2	−11.9
PS25PE75	321.8	11.8	−12.0
PS50PE50	317.3	13.5	−12.6
PS75PE25	319.1	12.7	−12.4

Table 4
VFT fit results for PP and its blends

	β_{PP}		
	T_v (K)	E_v (kJ/mol)	$\log(\tau_\infty)$
PP	168.3	28.6	−15.6
PS25PP75	162.6	29.0	−15.7
PS50PP50	163.5	30.1	−16.3
PS75PP25	184.6	22.5	−15.0
PP25PE75	164.7	31.6	−16.1
PP50PE50	183.9	24.4	−15.9
PP75PE25	178.9	25.4	−16.0

polymers, these processes were found to have different activation energies of 34.1 kJ/mol (β_{PS}) and 43.2 kJ/mol (γ_{PE}), respectively. For the blends, however, these individual processes overlapped strongly, resulting in the observation of a single relaxation maximum. Accordingly, the effective activation energies of this 'mixed' process fall in between those of the β_{PS} and γ_{PE} process. The intensity of these broad relaxation peaks is low, resulting in large scatter of the data points.

3.3.2.2. PS–PP blends. Fig. 9 shows the relaxation processes found for the PS–PP blends. The sub glass transition processes and the intra-crystalline α_{PP} process are not observed in PP and its blends. Similar to the PS–PE blends, there is virtually no effect of the blend composition on the glass transition dynamics of PS. The values of the VFT fit results are listed in Table 3.

In contrast, for all blend samples, the β_{PP} process reveals a slight, nevertheless significant speed-up of the relaxation times by a factor of two compared to pure PP. The VFT parameters and other details are listed in Table 4. In addition, the β_{PP} peak becomes broader with increasing PS content. This indicates an increase in mobility of the amorphous PP parts. The PP in the blends may become more heterogeneous than the pure PP.

The intermediate process, which is visible in the temperature range between 0.0022 and 0.0033 K^{-1} (190 and 30 °C), can again be related to the interfacial relaxation provoked by the electrical heterogeneity of the blend. Further inspection of the data reveals that the IFP process changes its temperature dependence upon crystallisation of PP: between 0.0022 K^{-1} (190 °C) and the crystallisation temperature of PP (0.0024 K^{-1} or 140 °C) the IFP relaxation obeys VFT behaviour that is likely governed by the mobility of the PP melt. Upon crystallisation of the PP phase, the effective conductivity of the PP fraction drops due to the formation of PP lamellae, which hamper ionic charge transport. As an indirect effect of crystallisation there might be additional changes in the conductivity of the remaining (inter-crystalline) amorphous PP phase due to constraints and confinement effects that affect the segmental mobility.

3.3.2.3. PP–PE blends. The cooperative β-relaxations of the two phases strongly overlap (cf. Figs. 4(b), 5(b) and 7) in the PP–PE blends. To evaluate the relaxation time and strength of the two phases in this case we applied the following two-step fit procedure.

In the first step, the two peaks are fitted separately, using the *a* and *b* parameters of the pure polymers. In a next step, the two computed HN-functions were added and the parameters $\Delta\varepsilon$, τ and *a* were adjusted to optimise the fit of the experimental spectrum. Here, the values of the parameter *b* were kept unchanged.

The efficiency of the multi-step fit procedure is demonstrated in Fig. 10, which shows two well-separated glass transition processes referring to the PP and PE blend fractions. Both processes reveal again only weak, if any, effects of the blend composition on the structural relaxation time. The VFT fit results of the PP and PE relaxation times are listed in Tables 4 and 5, respectively.

The intensities of the α_{PE} and γ_{PE} processes in the blends were too low for quantitative analysis and, therefore, they are not shown in Fig. 10. The relaxation times for the α process in pure PE are shown as a reference.

3.3.3. Relaxation strength

An essential outcome of previous work [17] was to show the linearity between the relaxation strength, $\Delta\varepsilon$ of the (amplified) glass transition process and the probe concentration, w_{probe}, in the concentration range from 0.1 to 1 wt%. Moreover, the normalised dielectric response $\Delta\varepsilon/w_{probe}$ turned out to be identical for all three different polymers (PE, PP and PS), indicating that all dissolved probe molecules contribute to the dielectric response in the specific concentration range.

Table 5
Arrhenius and VFT fit results for PE and its blends

	α_{PE}			β_{PE}		γ_{PE}	
	E_a (kJ/mol)	$\log(\tau_\infty)$	T_v (K)	E_v (kJ/mol)	$\log(\tau_\infty)$	E_a (kJ/mol)	$\log(\tau_\infty)$
PE	119.6	−23.7	169.5	19.1	−13.9	43.2	−18.8
PS25PE75	119.2	−23.0	167.7	19.1	−13.8	39.5	−16.8
PS50PE50	106.5	−21.1	170.6	19.1	−14.2	42.4	−16.4
PS75PE25	119.3	−23.0	165.7	19.2	−13.7	48.5	−19.5
PP25PE75			167.5	19.1	−13.7		
PP50PE50			164.3	19.4	−13.7		
PP75PE25			163.2	18.2	−12.9		

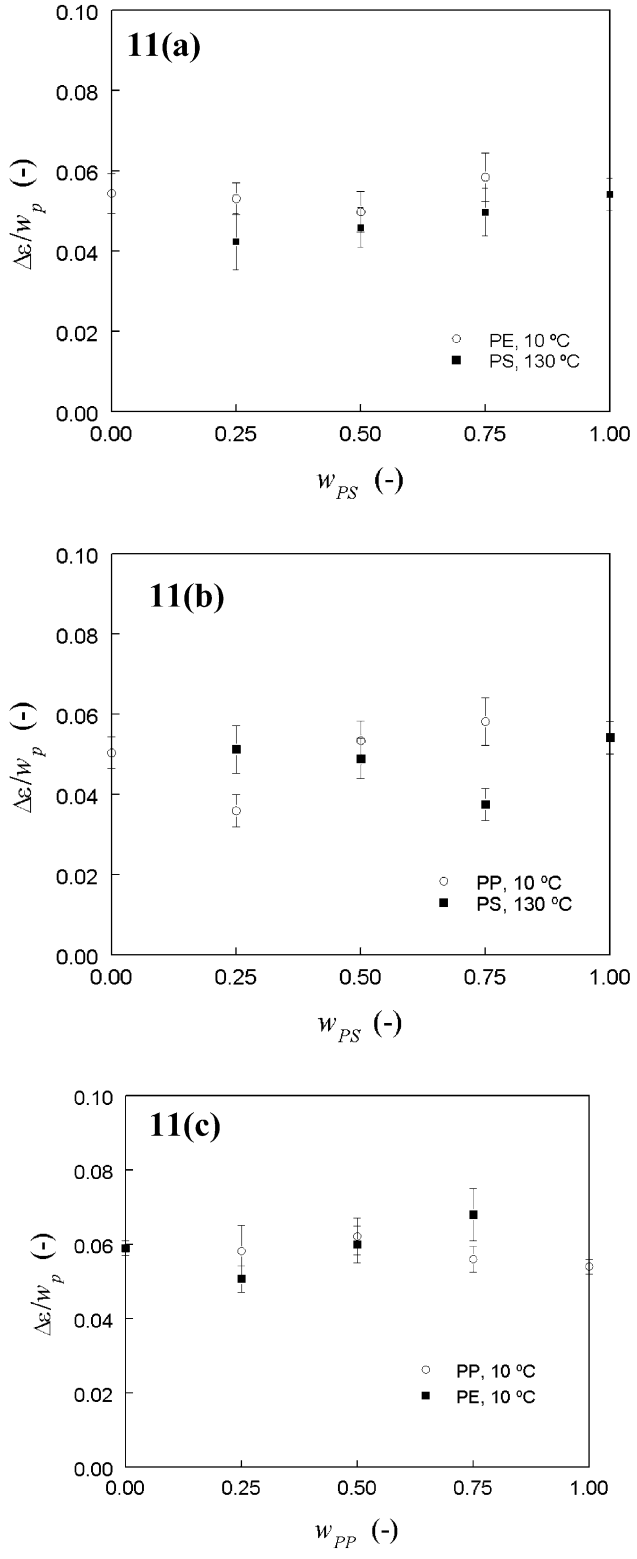

Fig. 11. Dielectric relaxation strength in the blends as a function of the composition of (a) PS–PE blends, (b) PS–PP blends and (c) PP–PE blends.

Using this finding, we are now in the position to determine the distribution of DBANS molecules over the two blend components from the relaxation strength of the individual glass transition processes. Fig. 11 shows the normalised relaxation strength of the two glass transition processes, i.e. $\Delta\varepsilon$ divided by the mass fraction of the polymer w_p, for each blend type and blend composition. Since, PS has an intrinsic α process of substantial intensity ($\Delta\varepsilon \sim 0.4$), we had to correct the experimental $\Delta\varepsilon$-values accordingly. As a result, all three blend types reveal nearly concentration independent $\Delta\varepsilon/w_p$ values within the experimental error, which is naturally higher for the data corresponding to the minor phase ($w_p = 0.25$). Furthermore, the $\Delta\varepsilon/w_p$ curves are not sensitive to the type of polymer, which proves that DBANS shows no preference to one of the blend components.

4. Conclusions

Dielectric relaxation spectroscopy using dielectric probes has been applied to study the (glass transition) dynamics in apolar polymers blends. By virtue of selective amplification of the cooperative relaxations related to the dynamic glass transition, we were able to obtain accurate relaxation data on the β_{PE}, β_{PP} and α_{PS} processes for three binary blend types and for a wide range of blend compositions.

No substantial influence of the blend composition and thus blend morphology on the glass transition dynamics was found, indicating that the blend constituents behave like homogeneous bulk materials. In other words, the relaxation times of the two phases and their temperature dependence correspond well to those of the pure polymers; a result that is to be expected for immiscible blends with structural dimensions on the micrometer scale.

The relaxation strength of the β_{PE}, β_{PP} and α_{PS} processes, normalised by the weight fraction of the respective polymer phase, revealed a constant value, regardless of the blend type and blend composition. This proves that the probe molecule, DBANS, is equally distributed in both components of all three blends of PE–PP, PE–PS and PP–PS.

These findings were tested using blends with partially overlapping relaxation dynamics. The behaviour of the two individual phases in PP–PE blends could be extracted by the summation of the two HN equations of the pure polymers.

This technique, therefore, allows quantitative analysis of complex systems, e.g. blends with overlapping glass transition dynamics or blends with simultaneous crystallisation and glass transition. In particular this is due to the easy measurement of the dynamics over large frequency and temperature range, which provides the identification of the various relaxation processes.

Acknowledgements

This work forms part of the research program #252 of the Dutch Polymer Institute (DPI). The authors want to thank

DSM Polypropylenes, Sabic Petrochemicals and Shell for the materials.

References

[1] Kremer F, Schönhals A, editors. Broadband dielectric spectroscopy. Berlin: Springer; 2002.
[2] Bottcher CJF, Bordewijk P, editors. Theory of electric polarization. New York: Elsevier; 1978.
[3] Hill NE, Vaughan WE, Price AH, Davies M, editors. Properties and molecular behaviour. London: Van Nostrand Reinhold; 1969.
[4] Runt JP, Fitzgerald JJ, editors. Dielectric spectroscopy of polymeric materials: fundamentals and applications ACS professional reference series, vol. 1. Washington: ACS Books; 1977. p. 329–78.
[5] McCrum NG, Read BE, Williams G, editors. Anelastic and dielectric effects in polymeric solids. New York: Dover Publications; 1967.
[6] Wübbenhorst M, de Rooij AL, van Turnhout J, Tacx J, Mathot V. Colloid Polym Sci 2001;279:525.
[7] Zetsche A, Fischer EW. Acta Polym 1994;45:168.
[8] Katana G, Fischer EW, Hack Th, Abetz V, Kremer F. Macromolecules 1995;28:2714.
[9] Hayakawa T, Adachi K. Macromolecules 2000;33:6834.
[10] Hayakawa T, Adachi K. Macromolecules 2000;33:6840.
[11] Karatasos K, Vlachos G, Vlassopoulos D, Fytas G, Meier G, Du Chesne A. J Chem Phys 1998;108:5997.
[12] Simon GP, Runt JP. In: Runt JP, Fitzgerald JJ, editors. Dielectric spectroscopy of polymeric materials: fundamentals and applications ACS professional reference series vol. 1. Washington: ACS Books; 1997. p.329–78.
[13] Boersma A, van Turnhout J, Wübbenhorst M. Macromolecules 1998; 31:7453.
[14] Wübbenhorst M, Folmer BJB, van Turnhout J, Sijbesma RP, Meijer EW. IEEE Trans Dielectrics Electr Insulat 2001;8:365.
[15] Ashcraft CR, Boyd RH. J Polym Sci, Polym Phys Ed 1976;14:2153.
[16] Frübing P, Blischke D, Gerhard-Multhaupt R, Khalil MS. J Phys D: Appl Phys 2001;34:3051.
[17] van den Berg O, Sengers WGF, Jager WF, Picken SJ, Wübbenhorst M. Macromolecules 2004;37:2460.
[18] Williams G, Hains PJ. Chem Phys Lett 1971;10:585.
[19] Dionisio MS, Mouraramos JJ, Williams G. Polymer 1994;35:1705.
[20] Livanova NM, Zaikov GE. Polym Degrad Stab 1997;57:1.
[21] This dipole moment was calculated with the Chem3D software package from Cambridge Software using the AM1 method in combination with a closed cell wave function and Mulliken charges.
[22] Wübbenhorst M, van Turnhout J. J Non-Cryst Solids 2002;305:40.
[23] van Turnhout J, Wübbenhorst M. J Non-Cryst Solids 2002;305:50.
[24] Brandrup J, Immergut EH, Grulke EA, editors. Polymer handbook. 5th ed. London: Wiley; 1999.
[25] Scott CE, Macosko CW. Polymer 1994;35:5422.
[26] Willemse RC, Posthuma de Boer A, van Dam J, Gotsis AD. Polymer 1998;39:5879.
[27] Sundararaj U. Macromol Symp 1996;112:85.
[28] Donth E. The glass transition. Relaxation dynamics in liquids and disordered materials. Berlin: Springer; 2001.
[29] Steeman P, van Turnhout J. In: Kremer F, Schönhals A, editors. Broadband dielectric spectroscopy. Berlin: Springer; 2002.
[30] Ngai KL, Rizos AK, Plazek DJ. J Non-Cryst Solids 1998;235:435.
[31] Forrest JA, DalnokiVeress K, Dutcher JR. Phys Rev E 1997;56:5705.
[32] Wübbenhorst M, Murray CA, Dutcher JR. Eur Phys J E 2003;12: S109.
[33] Boyd RH. Polymer 1985;26:323.
[34] Schmidt-Rohr K, Spieß HW. Macromolecules 1991;24:5288.